11 Superconductivity and Magnetism

L. Das, D. Sutter, O. Ivashko, D. Destraz, K. Kramer, D. Rechsteiner, C. E. Matt, J. Choi, M. Horio & J. Chang

in collaboration with: Paul Scherrer Institute (M. Dantz, Y .Tseng, D. E. McNally, N. Plumb, M. Shi, & T. Schmitt), EPFL Lausanne (G. Gatti, N. E. Shaik, H. M. Rønnow & M. Grioni), University of Zurich (F. Schindler, A. Cook & T. Neupert), University of Central Lancashire, UK (P. G. Freeman), Technical University of Denmark, Denmark (N. B. Christensen), Dipartimento di Fisica 'E. R. Caianiello', Salerno-Italy (F. Forte, V. Granata, R. Fittipaldi, M. Cuoco & A. Vecchione), The University of Tokyo, Japan (S. Pyon), Okayama University, Japan (K. Kudo & M. Nohara), Weizmann Institute of Science, Israel (M. Hücker), Deutsches Elektronen-Synchrotron DESY, Germany (M. von Zimmermann)

Our group is carrying out experimental research on strongly correlated electron systems using complementary synchrotron and laboratory based techniques. In this report, we highlight three different experiments. First, we have continued our work on the puzzling Mott insulating state of Ca_2RuO_4 by combining absorption and resonant inelastic x-ray spectroscopies. We have been able to reveal the intricate interplay between crystal-field and orbital degrees of freedom. Our second highlight is on a high-temperature superconductor where, by means of angle resolved photoemission, we have uncovered the orbital hybridisation at the Fermi level. It is discussed how this impacts on superconductivity. Finally, we have also studied the interplay between charge ordering and superconductivity in the $Ir_{1-x}Pt_xTe_2$ system.

11.1 Mott-Mechanism of Ca_2RuO_4 revealed

Spin-orbit coupling (SOC) is a central thread in the search for novel quantum material physics. A particularly promising avenue is the combination of SOC and strong electron correlations in multi-orbital systems. This scenario is realised in heavy transition metal oxides composed of 4*d* and 5*d* elements. Of particular interest is the complex regime where SOC and crystal-field energy scales are comparable. Here Ca_2RuO_4 is a topical material that displays a wealth of physical properties. Current-induced giant diamagnetic response (the strongest diamagnetism among non-superconducting materials) was recently reported [1]. Also, neutron and Raman scattering experiments have shown evidence for a dispersive Higgs mode [2, 3]. Experimental studies of angle-resolved photoemission spectroscopy and band structure calculations on the paramagnetic insulating phase of Ca_2RuO_4 have supported evidence for a band-Mott insulating ground state [4] due to interplay between Coulomb interaction and Hund's coupling. The rich and myriad phenomenology of Ca_2RuO_4 is hence attributed to various energy scales – Coulomb interaction U, Hund's coupling J_H, crystal-field splitting δ and SOC λ.

We have studied the magnetically ordered phase of Ca_2RuO_4 at $T = 16$ K, using O K edge Resonant Inelastic X-ray Scattering (RIXS) [5]. Four excitations have been identified – two low energy excitations labelled *A* and *B* at 80 meV and 400 meV respectively and two high energy excitations labelled *C* and *D* at 1.3 eV and 2.2 eV respectively as indicated in Fig. 11.1. The *A* and *B* branches are interpreted to be arising from composite spin-orbital excitations due to SOC and the high-energy excitations, dubbed *C* and *D*, arise from singlet-triplet excitations at the Ruthenium site set by energy scale of Hund's coupling.

A light polarisation analysis was carried out yielding information about the internal structure of these excitations. The momentum dependent analysis of the *A* and *B* peaks were made. Even though the dispersion of the

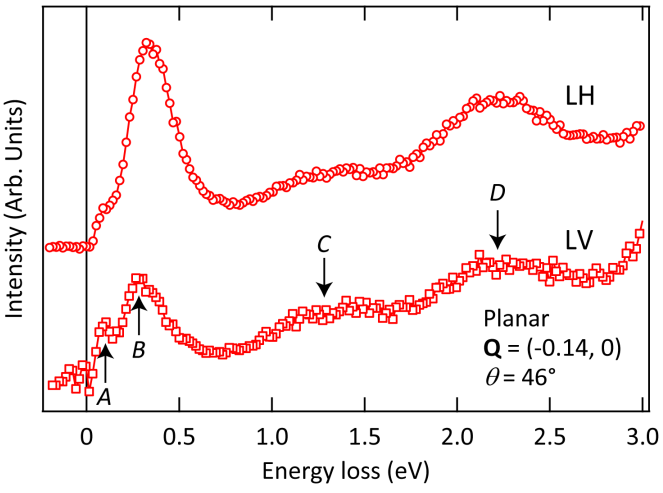

FIG. 11.1 – Planar RIXS spectra, recorded with LH and LV light polarisation for incident angle (momentum transfer) as indicated. The elastic scattering contribution is subtracted. Vertical arrows indicate the four excitations labelled *A*, *B*, *C* and *D*.

A peak was not discernible with our current resolution, the B peak showed a weak dispersion consistent with its propagating nature. Further, with the light polarisation analysis of the x-ray absorption and the RIXS spectra, we were able to characterise the Mott-active Ruthenium orbitals involved in the absorption processes. Our results are consistent with the picture of an almost completely filled d_{xy} orbital (becoming inaccessible to absorption processes) and half-filled $d_{xz/yz}$ orbitals involved in the Mott transition, thus, playing a pivotal role in creating the unique band-Mott insulating state of Ca_2RuO_4.

To understand the nature of the high energy excitations (C and D), a model cluster of two Ru sites connected to one planar oxygen site was used. The model was evaluated using material specific values of the energy scales: crystal field splitting $\delta = 0.3$ eV, SOC $\lambda = 0.075$ eV, Coulomb interaction $U = 2$ eV and Hund's coupling $J_H = 0.5$ eV. With this model, the spectral features named C and D were found to arise from singlet and triplet excitations at Ru site, with the energy given by $2J_H$ and $4J_H$, respectively. To describe the nature of the low-energy excitations (A and B), the eigenstates of the Hamiltonian of the single Ru site was considered and good agreement with the experimental data was obtained. In summary, we demonstrated that Ca_2RuO_4 is an example of a combined band-Mott insulator. The low-energy excitations of this ground state consists of damped dispersive spin-orbiton quasiparticles.

[1] C. Sow *et al.*, Science **358**, 1084 (2011)

[2] A. Jain *et al.*, Nat. Phys. **13**, 633 (2017)

[3] S.-M. Souliou *et al.*, Phys. Rev. Lett. **119**, 067201 (2017)

[4] D. Sutter *et al.*, Nat. Commun. **8**, 15176 (2017)

[5] L. Das *et al.*, Phys. Rev. X **8**, 11048 (2018)

11.2 Orbital Hybridisation in a Cuprate Superconductor

In the quest to improve superconducting transition temperatures in layered copper-oxide compounds (cuprates), it is important to identify the influencing factors of the transition temperature T_c. In single-layer cuprate superconductors, the particular crystal field environment of the copper oxide octahedra causes the nine $3d$-electrons to fill the t_{2g} manifold and leaves the e_g-states 3/4 filled [6]. Although superconductivity is promoted within the copper-oxide layers, the apical oxygen possibly plays a crucial role in defining T_c [7, 8]. The distance of the apical oxygen to the CuO_2-plane d_A then controls the hybridisation strength between the filled d_{z^2} -band and the metallic $d_{x^2-y^2}$ -band. Generally, in the single-layered materials T_c seems to correlate with larger d_A [9], thus suggesting

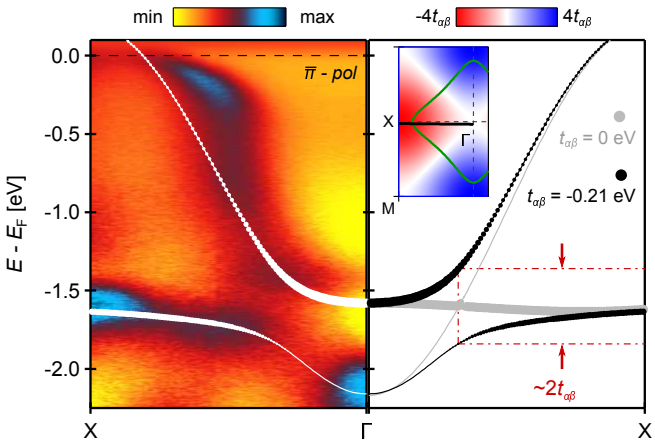

FIG. 11.2 – Avoided band crossing. Left panel: Ultraviolet ARPES data recorded along the anti-nodal direction using 160 eV linear horizontal polarised photons. Right panel: Tight-binding model of the $d_{x^2-y^2}$ and d_{z^2} bands along the anti-nodal direction. The gray lines are the model prediction in absence of inter-orbital hopping ($t_{\alpha\beta} = 0$) between $d_{x^2-y^2}$ and d_{z^2}. In this case, the bands are crossing near the Γ-point. This degeneracy is lifted once a finite inter-orbital hopping parameter is considered. For the solid black lines $t_{\alpha\beta} = -210$ meV and other hopping parameters have been adjusted accordingly. The inset indicates the Fermi surface (green line) and the Γ−X cut directions. The coloured background displays the amplitude of the hybridisation term $\Psi(\mathbf{k})$ that vanishes on the nodal lines.

a sabotaging role of orbital hybridisation for superconductivity. However, the d_{z^2} -band has never been directly identified by angle-resolved photoemission spectroscopy (ARPES) studies.

In a recent experiment [10], we have resolved the d_{z^2}-band in La-based single-layer compounds with ultraviolet and soft X-ray ARPES measurements. We have pinned down the orbital character in three different ways. Firstly, our observations are consistent with density functional theory (DFT) calculations, suggesting the existence of the d_{z^2}-band below the $d_{x^2-y^2}$-band. Secondly, by using matrix element selection rules of the optical transition we can test the orbital character by varying the measurement geometry and light polarisation [11]. The incident light and the electron detector slit define a global mirror-plane. With respect to this plane one can assign the parity for the electromagnetic light field and the parity of the orbitals. For the free electron final state (even parity), the selection rules dictate if the photocurrent for a certain orbital-driven band vanishes or not. Thirdly, using soft X-rays, we were able to probe the band structure in k_z-direction and observed dispersive features of the d_{z^2}-band beyond matrix element effects, in contrast to the non-dispersive $d_{x^2-y^2}$-band.

Experimental data and DFT results have been parametrised using a two-orbital tight binding model [11]. Crucially, there is a hybridisation term $\Psi(\mathbf{k}) = 2t_{\alpha\beta}[\cos(k_x a) - \cos(k_y b)]$ between the $d_{x^2-y^2}$ and d_{z^2} orbitals, with the hopping parameter $t_{\alpha\beta}$ that characterises the strength of orbital hybridisation. If one describes the two observed bands independently with $t_{\alpha\beta} = 0$, they would cross each other along the antinodal (Γ–X) direction which is not observed experimentally (see Fig. 11.2). From the avoided band crossing, we directly estimate a hybridisation term of $t_{\alpha\beta} \approx 200$ meV. Furthermore, in contrast to the widely used single-band tight binding parametrisation, our two-band model allows a unification of t'_α/t_α ratios for all single-layer compounds, where t_α is the nearest neighbour hopping and t'_α is the next nearest neighbour hopping for the $d_{x^2-y^2}$ orbitals. It has been argued that orbital hybridisation - of the kind reported here - is unfavourable for superconducting pairing [7,12]. It thus provides an explanation for the varying $T_c^{\max}$ across single-layer cuprate materials.

[6] J. Fink *et al.*, J. Res. Dev. **33**, 372 (1989)

[7] H. Sakakibara *et al.*, Phys. Rev. Lett. **105**, 057003 (2010)

[8] Y. Ohta *et al.*, Phys. Rev. B **43**, 2968-2982 (1991)

[9] E. Pavarini *et al.*, Phys. Rev. Lett. **87**, 047003 (2001)

[10] C. Matt, D. Sutter *et al.*, Nat. Commun. **9**, 972 (2018)

[11] C. B. Bishop *et al.*, Phys. Rev. B **93**, 224519 (2016)

[12] H. Sakakibara *et al.*, Phys. Rev. B **85**, 064501 (2012)

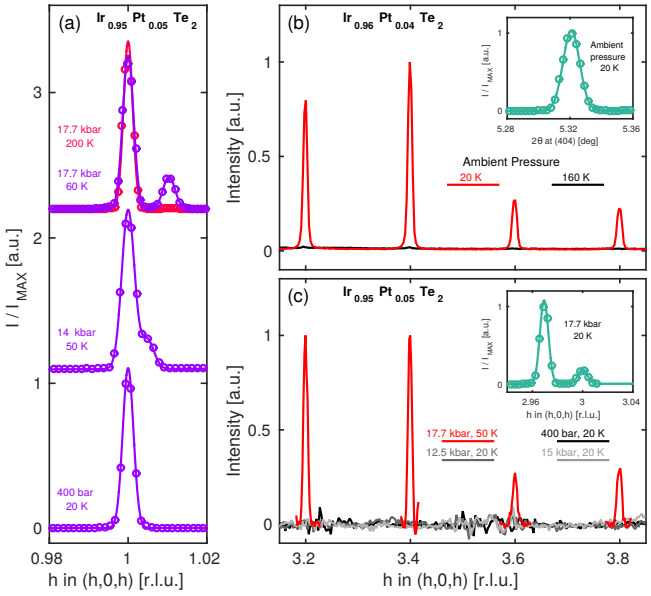

FIG. 11.3 – Lattice and charge ordering reflections in $Ir_{1-x}Pt_xTe_2$. (a) Bragg peak $(1,0,1)$ reflection measured in $Ir_{0.95}Pt_{0.05}Te_2$ as a function of pressure as indicated. Solid lines are Gaussian fits to the data. (b) Ambient pressure x-ray diffracted intensity measured on $Ir_{0.96}Pt_{0.04}Te_2$ along the $(1,0,1)$ direction for 20 K (red line) and 160 K (black line) respectively. (c) Scan as in (b) but measured at base temperature (20 K) on $Ir_{0.95}Pt_{0.05}Te_2$ for pressures as indicated. The slightly worse signal-to-noise level stems from the necessary background subtraction of signal originating from the pressure cell.

11.3 Charge-Stripe Order and Superconductivity in $Ir_{1-x}Pt_xTe_2$

$IrTe_2$ is an interesting system because of a large SOC on the Ir site [13, 14]. It also displays high-temperature charge ordering, and superconductivity can be induced by Pt or Pd substitution that in turn quenches the charge order [15–17]. Several studies concluded in favour of a conventional *s*-wave pairing symmetry [18,19]. It remains however to be understood how charge order, lattice symmetry and superconductivity interfere. In the parent compound $IrTe_2$, charge order coincides with a lowering of the crystal structure symmetry (from hexagonal $P\bar{3}m1$ to monoclinic $C2/m$) [15].

We carried out a combined resistivity and x-ray diffraction study of $Ir_{1-x}Pt_xTe_2$, as a function of chemical substitution and hydrostatic pressure near the critical composition $x_c \sim 0.045$ [20]. Just below this critical composition, we find a temperature independent charge ordering modulation vector $(1/5, 0, 1/5)$ (see Fig. 11.3(b)). This signifies a difference from the parent compound where the ground state charge modulation is $(1/8, 0, 1/8)$ [21]. Our pressure experiments were carried out just above x_c (namely at $x = 0.05$) in a compound with a superconducting ground state and no evidence of charge order at, and around, ambient conditions $1 - 400$ bar. With increasing pressure, we find a lowering of lattice symmetry, evidenced by a Bragg peak splitting above $p_{c1} \sim 11.5$ kbar (see Fig. 11.3(a)). This breaking of the hexagonal lattice symmetry appears without any trace of charge ordering that emerges only for pressures above $p_{c2} \sim 16$ kbar (see Fig. 11.3(c)). Since the charge ordering is intimately related to the shorter lattice parameter (inset of Fig. 11.3(c)), we conclude that charge ordering is lattice – rather than electronically – driven.

We also dealt with the interplay between charge ordering and superconductivity. The temperature versus Pt substitution phase diagram suggests that these two phases are competing, since superconductivity appears only after charge ordering is quenched. From resistivity data we observe a gradual broadening of the transition (as a function of pressure for $x = 0.05$ system), to a point where zero resistance is not observed. This is consistent with Kosterlitz-Thouless transition [22, 23] scenario where an exponential drop in resistivity is predicted. In $Ir_{1-x}Pt_xTe_2$ it is know that charge order generates two

dimensional walls of low density-of-states [24, 25]. It is therefore not inconceivable that superconductivity is suppressed inside these walls. Hence there exists a possible physical mechanism for two-dimensional superconductivity in $Ir_{1-x}Pt_xTe_2$. Further experimental evidence supporting this scenario would be of great interest. Another plausible scenario to describe the broad resistive transition is granular superconductivity. We notice, however, that the pressure induced crystal domain formation initially have no influence on superconductivity. Explaining our data in terms of granular superconductivity is therefore not straightforward.

[13] B. J. Kim *et al.*, Phys. Rev. Lett. **101**, 076402 (2008)
[14] M. Moretti Sala *et al.*, Phys. Rev. B **89**, 121101 (2014)
[15] S. Pyon *et al.*, J. Phys. Soc. Jpn. **81**, 053701 (2012)
[16] J. Yang *et al.*, Phys. Rev. Lett. **108**, 116402 (2012)
[17] S. Pyon *et al.*, Physica C **494**, 80 (2013)
[18] S. Y. Zhou *et al.*, Europhys. Lett. **104**, 27010 (2013)
[19] D. J. Yu *et al.*, Phys. Rev. B **89**, 100501 (2014)
[20] O. Ivashko *et al.*, Sci. Rep. **7**, 17157 (2017)
[21] K.-T. Ko *et al.*, Nat. Commun. **6**, 7342 (2015)
[22] Q. Li *et al.*, Phys. Rev. Lett. **99**, 067001 (2007)
[23] L. Benfatto *et al.*, Phys. Rev. B **80**, 214506 (2009)
[24] G. L. Pascut *et al.*, Phys. Rev. Lett. **112**, 086402 (2014)
[25] G. L. Pascut *et al.*, Phys. Rev. B **90**, 195122 (2014)